Fuel 289 (2021) 119868

Contents lists available at ScienceDirect

Fuel

journal homepage: www.elsevier.com/locate/fuel

Full Length Article

Numerical modelling of sorption-enhanced gasification: Development of a fuel decomposition model

Antti Pitkäoja [a,*], Jouni Ritvanen [a], Selina Hafner [b], Timo Hyppänen [a], Günter Scheffknecht [b]

[a] Lappeenranta-Lahti University of Technology, LUT School of Energy Systems, P.O. Box 20, FI-53851 Lappeenranta, Finland
[b] Institute of Combustion and Power Plant Technology (IFK), University of Stuttgart, 7 Pfaffenwaldring 23, 70569 Stuttgart, Germany

ARTICLE INFO

Keywords:
Sorption-enhanced gasification
Gasification
Biomass
Thermochemical conversion
Pyrolysis
Simulation

ABSTRACT

Sorption-enhanced gasification (SEG) is a promising technology for producing renewable feedstock gas to be used in biofuel synthesis processes, especially in dimethyl ether (DME) synthesis. To adopt the technology on a commercial scale, it is necessary to acquire knowledge about the related operational characteristics. The SEG process is carried out at lower temperatures than those employed in conventional gasifiers. A typical operating range is from 600 °C to 800 °C. Fuel decomposition experiments have shown distribution of the decomposition products to vary by the process temperature in this operating range, and thus, it is important to adapt this phenomenon for modelling the SEG process. To model the temperature dependence of the decomposition products, a fuel model was developed. Fuel decomposition experiments were conducted to obtain the boundary conditions for the fuel model. The developed fuel model was implemented to an SEG model frame, and the model prediction was compared against data from a 200 kW_{th} dual fluidised bed facility. The model gave satisfactory predictions for producer composition and temperature trends. Furthermore, the main balances of the model were in agreement with typical trends of the SEG process. The conducted simulations improved our understanding of material balances in SEG reactors. Knowledge from physical operations governing the process is of value in further development of the technology.

1. Introduction

Increased greenhouse gas emissions during the past few decades have induced the European Union (EU) to pursue a climate policy whose goal is to keep average global warming below 2 °C compared to pre-industrial temperatures [1]. To pursue this policy, the EU has set a target of 14% renewable energy usage for the transportation sector by 2030 [2]. Consequently, there is a pressing need to develop effective and cost-efficient ways for producing transportation fuels from renewable sources. The transportation sector has relied on liquid fossil oil-derived fuels, such as petroleum and diesel, for decades. A cost-efficient alternative is thus to replace fossil-based diesel fuel with liquefied renewable dimethyl ether (DME).

Sorption-enhanced gasification (SEG) has been recognised as a promising technology to produce renewable feedstock for the synthesis of DME. The SEG process operated within specific operating conditions can produce a feedstock gas from biomass that is almost directly suitable for the DME synthesis. This has been experimentally verified under a certain operating condition of the gasifier [3]. The benefit of the process is that additional downstream modification of the producer gas composition is not required. In the SEG process, the producer gas composition can be tailored to be suitable for the downstream DME synthesis in the gasification reactor.

However, experiments are usually limited to a finite number of experimental points; operations outside the experimental points or on a different scale cannot be evaluated with certainty. To overcome these experimental limitations, a process model can be developed. Process modelling can directly evaluate the impact of various process parameters on the operation of a gasifier. To develop a process model for this purpose, the main phenomena governing the operation of the process must be included in the model. Occasionally, a simplified gasification process model with only the most relevant characteristics has been sufficient to produce satisfactory prediction capability [4]. However, in other instances, more detailed modelling approaches have been developed, especially for fuel decomposition [5,6].

The fuel decomposition process is called pyrolysis, and it is the primary step of biomass gasification. During pyrolysis, the biomass is decomposed into solid and gaseous fractions. The gas fraction is formed from non-condensable and condensable gas species. The condensable

* Corresponding author.
E-mail address: antti.pitkaoja@lut.fi (A. Pitkäoja).

https://doi.org/10.1016/j.fuel.2020.119868
Received 20 August 2020; Received in revised form 13 November 2020; Accepted 25 November 2020
Available online 16 December 2020

Nomenclature

γ	parameter, [–]
ρ	density, [kg/m^3]
ar	as-received
C	concentration, [mol/m^3]
$C_{CO_2,eq}$	CO_2 equilibrium concentration, [mol/m^3]
ds	dry solid
dW	mass fraction difference, [kg$_i$/kg$_y$]
F	fuel
g	gas
H	reaction heat, [kJ]
i	index
j	index
k	chemical reaction rate coefficient, [1/s]
k'	chemical reaction rate coefficient, [m^3/(mol·s)]
K_{WGS}	water–gas shift equilibrium coefficient, [–]
M	molar mass, [g/mol]
n	mole, [mol]
PG	permanent gas
Q	energy, [J]
R	reaction rate, [kg/(m^3·s)]
R_i	ideal gas constant, [J/(mol·K)]
s	solid
T	temperature, [K]
W	mass fraction, [kg$_i$/kg$_y$]
y	mol fraction, [mol$_i$/mol$_y$]

fraction is mainly formed from heavy hydrocarbons, referred to as tars.

In the literature, there are several studies concerning fuel decomposition, and one of the main observations of these studies has been that the decomposition products vary by temperature [7]. A comprehensive literature review concerning fuel decomposition products was made by [8]. The authors thoroughly reviewed many experimental studies for various biomasses and provided many examples of how the fuel decomposition products are changed by the process temperature.

Conventionally, fuel decomposition products have been modelled by using standard proximate analysis. Standard proximate analysis represents the fuel decomposition products at 905 °C. The standard approach has been successfully applied for conventional gasification processes, which are carried out at temperatures around 850 °C. In gasification processes that are carried out well below the conventional operating temperatures, the fuel decomposition products are expected to differ from those observed under standard characterisation conditions. The distribution of decomposition products is temperature-dependent, and it varies with temperature. To analyse low-temperature systems, this characteristic must be considered, and thus, a temperature-dependent fuel decomposition model is needed.

The goal of this study is to develop a fuel decomposition model suitable for low-temperature biomass gasification and to implement the model into an SEG model frame. By introducing characteristics of the decomposition phenomena into the model frame, the fuel model development is premised on the main characteristics of the decomposition process. The major decomposition products, e.g. permanent gases, char, and tar, are included in the model. Elemental balances are formulated based on these main products. The effect of temperature on the distribution of the main products is considered to model the effect of temperature on the elemental balances.

The fuel model is implemented into a previously published SEG model frame [9], and the model prediction is compared against gasification experiments [3]. In addition, fuel decomposition experiments were conducted at a temperature range that is important for the SEG process. The experiments were carried out to obtain boundary conditions for the fuel decomposition sub-model.

2. Numerical model development

Gasification can be divided into three major steps: drying, decomposition, and gasification of the decomposition products. A simplified overview of the gasification process is shown in Fig. 1. The objective of this work is to develop a fuel model that considers the main aspects of fuel decomposition. Fuel decomposition is one of the main process steps of gasification, and hence, it impacts the final gasification products.

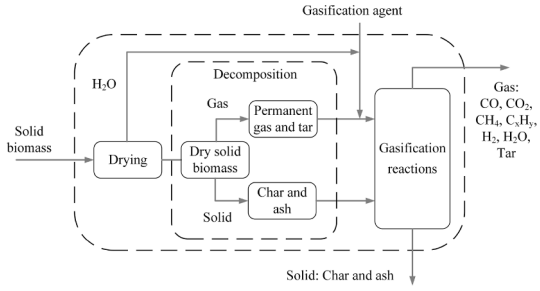

Fig. 1. Simplified process steps of gasification.

2.1. Drying

Biomass drying is carried out at low temperatures. The water bound in the biomass is analysed by drying the biomass. Determining the water fraction is a standard procedure belonging to the standard proximate analysis of the fuel.

2.2. Fuel decomposition

In fuel decomposition, the biomass is fractioned into solid and gas fractions. The gas fraction is formed from permanent gases (CO, CO_2, H_2, CH_4, and C_2–C_4 hydrocarbons) and condensable gas species, referred to as tars. The primary decomposition occurs at temperatures from 200 °C to 500 °C [8]. Typically, at temperatures around 500 °C, tar yield is maximised. At higher temperatures, the tar yield decreases owing to tar reformation reactions. The tars are decomposed to lower hydrocarbons, and in the process, additional permanent gases are released. This process continues until the decomposition temperature is approximately 905 °C. At this temperature, the fuel decomposition is free from the tars according to the standard proximate analysis.

A solid fraction is formed from biomass after the biomass is stripped from the volatile substances. The solid is formed from char and ash. The ash fraction of biomass is inert and is mainly formed from various trace elements. However, the char fraction varies by the process temperature [8]. The char inherits the same elements that were present in the parent fuel, and the elemental composition varies by the process temperature. According to [8], the char formed at decomposition is mostly formed from elemental carbon. However, there are still significant traces of hydrogen and oxygen present. In addition, low quantities of nitrogen and sulphur remain in the formed char [10].

2.3. Gasification reactions

The chemical reactions can be divided to reactions with char, permanent gases, and reaction with tars [11]. The main heterogenous reactions with the char are Boudouard, water–gas, and methanation reactions. The primary homogeneous reaction is water–gas shift reaction. Furthermore, there are various reaction paths for the decomposition of the tars. The tars are typically reduced to permanent gases by oxidation, dry reforming, steam reforming, hydrogenation, and thermal cracking reactions. These reactions can be homogeneous or heterogeneous, and they can take place inside or outside the biomass particles. The tar reactions are not commonly modelled owing to very complex reaction networks and uncertainty about the application of reaction networks to the fluidised bed process.

2.4. Main modelling assumptions and formulation of decomposition balances

A fuel model that considers the most significant fractions of the fuel and their temperature-dependent interrelations is developed. The main assumptions of the fuel decomposition model are as follows:

- Fuel is decomposed to permanent gases, tars, char, ash, and moisture.
- The relationship between permanent gases, tars, and char depends on temperature.
- The elemental composition of the main fractions are as follows:
  - Permanent gas (C, H, O, N, S)
  - Char (C, H, O, N, S)
  - Tar (C, H)
- Devolatilisation product gases from the fuel model are CO, CO_2, CH_4, C_2H_4, H_2S, NH_3, and H_2.
- Lower hydrocarbons (C_2–C_4) are lumped under the C_2H_4 model component.
- Tars are lumped under the single model component C_7H_8.
- All hydrocarbons are formed upon fuel decomposition, and are assumed as inert gas species without chemical reactions associated with the gases.
- Char gasification releases elements bound to the char as H_2S, H_2, O_2, and N_2.
- Fuel decomposition is instantaneous.
- Ash is an inert fraction.
- The ash and moisture fractions are based on the standard proximate analysis.

The hydrocarbons are assumed to be inert, and no reaction paths are associated with them. Elemental composition of hydrocarbons (CH_4, C_2-C_4 and tars) measured from producer gas is set into decomposition model for the hydrocarbon model components. This approach assures that the elemental distribution of hydrocarbons in the producer gas is according to measurements at the outlet of the gasifier. Fuel decomposition balances are formulated based on the assumptions presented above. According to the standard proximate analysis, the fuel is formed from four main fractions:

$$W_{F,ar} = W_{Vol,ar} + W_{Char,ar} + W_{Ash,ar} + W_{Moist,ar}, \quad (1)$$

where the fuel is the sum of the volatile, char, ash, and moisture fractions. The equation can be extended for a gasification process:

$$W_{F,ar} = W_{PG,ar} + W_{Tar,ar} + W_{Char,ar} + W_{Ash,ar} + W_{Moist,ar} \quad (2)$$

in which the tar fraction is separated from the volatile fraction. The fuel and the decomposition products can be divided into i elements:

$$\sum_i W_{F,daf,i} = \sum_i W_{PG,i} + \sum_i W_{Tar,i} + \sum_i W_{Char,i} \quad (i = C, H, O, N, S) \quad (3)$$

in which the sum of the elements makes up the main products and the fuel is formed from the sum of the main products or from the elements within the fuel. It should be noted that tar consists only of C and H elements. The char elemental composition is modelled according to [8] and [10]. Correlations for the C and H compositions of the char are according to [8]

$$W_{Char,C} = 0.93 - 0.92\exp(-0.0042T) \quad (4)$$

$$W_{Char,H} = -0.0041 + 0.1\exp(-0.0024T), \quad (5)$$

where T is fuel decomposition temperature in °C. Elements N and S are assumed to follow correlations by [10].

$$W_{Char,N} = 0.088 W_{F,N} W_{Char,daf}^{0.6} \left(\frac{W_{F,N}}{W_{F,C}}\right)^{-0.6} \quad (6)$$

$$W_{Char,S} = 0.14 W_{F,S} W_{Char,daf}^{0.2} \left(\frac{W_{F,H}}{W_{F,C}}\right)^{-0.6}, \quad (7)$$

where $W_{F,i}$ is the fraction of an element of the char's parent fuel according to the ultimate analysis. Oxygen represents the most uncertainty in data by [8], and therefore, O is resolved from the balance and the other elements from the correlations.

2.5. Tar fraction

The tar fraction is specified in the model as the mass fraction based on the tar measurement of the producer gas. Tar species that are measured from the producer gas are typically formed from elemental carbon and hydrogen [12]. Toluene (C_7H_8) was evaluated to represent the overall elemental composition of tars.

2.6. Volatile release

Volatile release is resolved from elemental mass balances by removing the char and the tar from the elemental composition of the fuel. The volatilised gas species are formed from the leftover elemental mass balance. The volatile composition follows stoichiome try.

$$y_C + y_H + y_O + y_N + y_S = y_{PG} = y_{NH_3} + y_{H_2S} + y_{CO} + y_{CO_2} + y_{CH_4} + y_{C_2H_4} + y_{H_2} \quad (8)$$

The volatile composition changes by temperature [8]. In the model, the stoichiometry can be altered with parameters γ_1 and γ_2.

$$\gamma_1 = \frac{n_{CO}}{n_{CO} + n_{CO_2}} \quad (9)$$

$$\gamma_2 = \frac{n_{CH_4,C}}{n_{CH_4,C} + n_{C_2H_4,C}} \quad (10)$$

The parameter γ_1 divides volatilized oxygen between CO and CO_2.

$$y_{O,CO} = \gamma_1 y_O \quad (11)$$

$$y_{O,CO_2} = 2(1-\gamma_1) y_O \quad (12)$$

The amount of oxygen determines carbon consumed by CO and CO_2 gases. The remaining carbon is consumed by CH_4 and C_2H_4 gases.

$$y_{C,rem} = y_C - y_{C,CO} - y_{C,CO_2} \quad (13)$$

$$y_{C,CH_4} = \gamma_2 y_{C,rem} \quad (14)$$

$$y_{C,C_2H_4} = (1-\gamma_2) y_{C,rem} \quad (15)$$

Elemental balances for the volatilised elements can be written as follows:

$$
\begin{aligned}
y_S &= y_{S,H_2S} \\
y_N &= y_{N,NH_3} \\
y_O &= y_{O,CO} + y_{O,CO_2} \\
y_C &= y_{C,CO} + y_{C,CO_2} + y_{C,CH_4} + y_{C,C_2H_4} \\
y_H &= y_{H,H_2S} + y_{H,NH_3} + y_{H,CH_4} + y_{H,C_2H_4} + y_{H,H_2}.
\end{aligned} \tag{16}
$$

Volatilised permanent gases are determined from the elemental balances.

2.7. Heat balance

The heat balance of the fuel decomposition is formulated based on theoretical reaction energies. The heat balance is modelled according to the following equations:

$$Q_{Reaction} = Q_{F,LHV} + Q_{F,H_2O} + Q_{Decomposition} \tag{17}$$

in which $Q_{F,LHV}$ is the lower heating value of fuel, Q_{F,H_2O} is evaporation of water, $Q_{Decomposition}$ is an external heat required by the decomposition and $Q_{Reaction}$ is combustion energy of decomposition products according to equation:

$$Q_{Reaction} = \sum_i W_{Char,i} Q_{Char,i} + \sum_j W_{PG,j} Q_{PG,j} + W_{Tar} Q_{Tar} \tag{18}$$

in which $W_{Char,i}$ is mass fraction of an char element, $W_{PG,j}$ is mass fraction of a gas specie, $Q_{Char,i}$ and $Q_{PG,j}$ are reaction heats of char elements and permanent gases, respectively. The energy balance is described in Fig. 2.

2.8. Overall balances of fuel model

The overall balances of the developed fuel model are summarised in Fig. 2. The mass and heat balances for fuel decomposition at 710 °C are presented. An example case based on a simulation is shown. Decomposition balances of fuel from the as-received state to individual gas species and solid char are presented.

2.9. Chemical reactions

Chemical reactions used in the model are summarised in Table 1. Chemical reactions are based on literature correlations for individual

Table 1
Chemical reactions.

Reaction	Equation	H (at 25 °C)	Ref.
Calcination	$CaCO_3(s) \rightarrow CaO(s) + CO_2(g)$		
	$R_{calc} = \rho_s k'_{calc} W^{2/3}_{s,CaCO_3} (C_{CO_2,eq} - C_{CO_2})$	178.3	[13–15]
	$k'_{calc} = 2057 \exp(-\frac{112400}{R_i T})$		
Carbonation	$CaO(s) + CO_2(g) \rightarrow CaCO_3(s)$		
	$R_{carb} = \rho_s k'_{carb} (W_{s,max} - W_{s,CaCO_3})(C_{CO_2} - C_{CO_2,eq})$	−178.3	[15–17]
	$k'_{carb} = 30$		
Sulphation	$CaO(s) + SO_2(g) + 0.5O_2(g) \rightarrow CaSO_4(s)$		
	$R_{sulph} = \rho_s W_{s,CaO} k_{sulp} W_{g,SO_2} W_{g,O_2}$	−502.1	[18]
	$k_{sulph} = 4.0(-3.843T + 5640)\exp(-\frac{8810}{T})$		
De-sulfation	$CaSO_4(s) + CO(g) \rightarrow CaO(s) + SO_2(g) + CO_2(g)$		
	$R_{desulph} = \rho_s W_{s,CaSO_4} k'_{desulp} C_{CO} A_{r,CaSO_4} M_{CaSO_4}$	219.2	[10]
	$k'_{desulph} = 0.005 \exp(-\frac{10000}{T})$		
Direct sulfation	$CaCO_3(s) + SO_2(g) + 0.5O_2(g) \rightarrow CaSO_4(s) + CO_2(g)$		
	$R_{disulph} = \rho_s W_{s,CaCO_3} k'_{disulp} C^{0.9}_{SO_2} C^{0.75}_{CO_2} C^{0.001}_{O_2} A_{r,CaCO_3} M_{CaCO_3}$	−323.8	[10]
	$k'_{disulph} = 0.01 \exp(-\frac{3031}{T})$		
Boudouard	$C(s) + CO_2(g) \rightarrow 2CO(g)$		
	$R_{boud} = k_{boud} \rho_{char} W_{char,C}$	172.4	[19]
	$k_{boud} = 2.11 \cdot 10^7 \exp(-\frac{219000}{R_i T}) p^{0.36}_{CO_2}$ [bar]		
Water –gas	$C(s) + H_2O(g) \rightarrow CO(g) + H_2(g)$		
	$R_{wg} = k_{wg} \rho_{char} W_{char,C}$	131.3	[20]
	$k_{wg} = 1.23 \cdot 10^7 \exp(-\frac{198000}{R_i T}) p^{0.75}_{H_2O}$ [atm]		
Methanation	$C(s) + 2H_2(g) \rightarrow CH_4(g)$		
	$R_{meth} = k_{meth} \rho_{char} W_{char,C}$	-75.0	[5]
	$k_{meth} = 16.4 \exp(-\frac{94800}{R_i T}) p^{0.93}_{H_2}$ [MPa]		
Water –gas shift	$CO(g) + H_2O(g) \leftrightarrow H_2(g) + CO_2(g)$		
	$R_{wgs} = M_{CO} k'_{wgs} ((C_{CO} C_{H_2O}) - (C_{CO_2} C_{H_2})/K_{wgs})$	−41.1	[21,22]
	$k'_{wgs} = 2.78 \exp(-\frac{3965}{T})$		

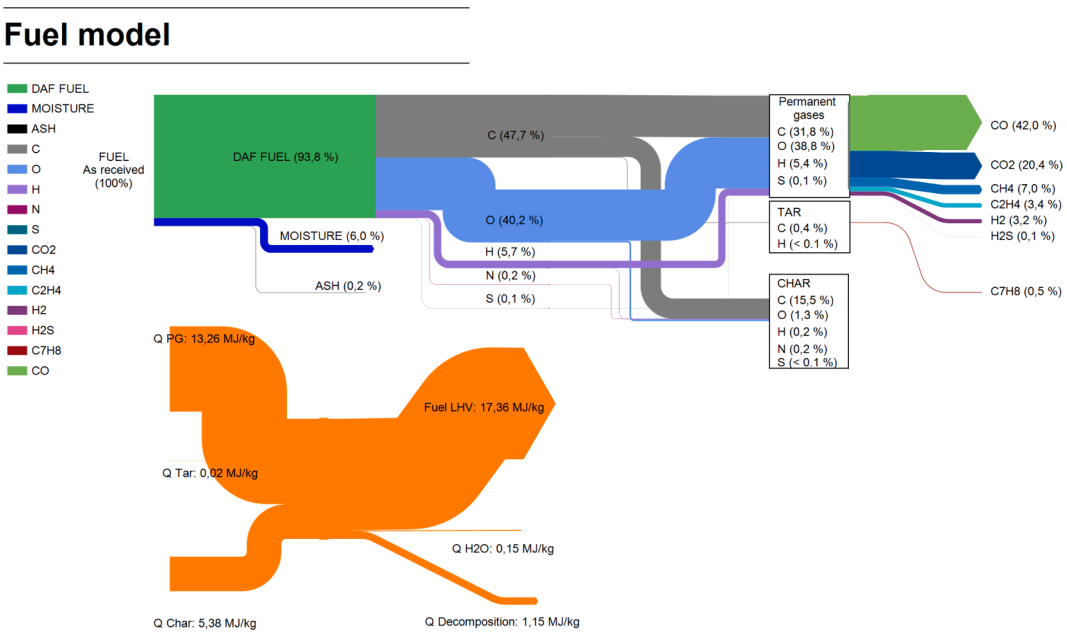

Fig. 2. Mass and heat balances of fuel model at 710 °C with $\gamma_1 = 0.764$ and $\gamma_2 = 0.642$.

chemical phenomena. Homogeneous and heterogeneous reactions are modeled as source terms of gas and solid phase mass balances. The balance equations and the main assumptions concerning the modelling of the chemical reactions in an SEG reactor are described elsewhere [9].

3. Experimental work

New experimental work focused on fuel decomposition was conducted to support the modelling. The experiments were carried out in the temperature range of 600–800 °C, which is the most relevant range for the SEG process. Wood pellets of the SEG gasification experiments were used to obtain proper boundary conditions for the fuel model. A brief description regarding the SEG gasification experiments is provided in this paper. The gasification experiments have been published in detail elsewhere [3].

3.1. Fuel decomposition experiments

Proximate analyses for wood pellets were carried out with a fixed bed reactor at temperatures of 650 °C, 700 °C, 750 °C, and 800 °C under atmospheric pressure. Wood pellets of ENplus A1-quality were used in the experiments. The mass of a single pellet was 15 g. The elemental composition of the pellets is presented in Table 2. The mass balances of the experiments are based on the fractions recovered from the reactor. The balances are shown in Table 3. The yields of the fractions are listed as received-based. Therefore, the liquid and solid yields in the table include the moisture and ash present in the fuel. The closures of the mass balances are reported as the sum of the measured fractions. The mass balances of the experiments were determined using the following procedure. The reactor was flushed by known N_2 flow, and the N_2 and other gases were collected in a bag. The permanent gas yield from the wood pellets was determined from a balance after gas chromatography analysis of the collected gases. The solid fraction was collected from the reactor after cooling. The liquid fraction was determined by weighing a condenser and various parts of the reactor where the liquid fraction can condense.

The permanent gas and liquid yields of the experiments represent the total volatile yield. The liquid fraction is formed from liquid organics and water, and it represents the tar fraction of the fuel [8]. The solid fraction is formed during devolatilisation. The solid fraction is in a stable state unless a reactive gasification agent is fed into the reactor. Distribution of the volatiles into the permanent gases and liquid varies by process conditions. The mass of the tar that is measured from a fluidised bed environment is much lower than from the fuel decomposition experiment. Therefore, the fraction given in Table 3 cannot be directly utilised in simulations of a fluidised bed without implementing reaction paths to decompose the tars to lighter gases. However, the solid fraction of the fuel from the experiments can be utilised in the analysis of a fluidised bed reactor.

3.2. Sorption-enhanced gasification experiments

Gasification experiments were conducted at a 200 kW_{th} dual fluidised bed (DFB) pilot facility at the Institute of Combustion and Power Plant Technology (IFK) at the University of Stuttgart [3]. The pilot facility consisted of a bubbling fluidised bed gasifier and a circulating fluidised bed combustor that were connected to each other. The pilot facility is shown in Fig. 3. Detailed information regarding the pilot facility is provided in [9]. The experimental work focused on varying the temperature of the SEG pilot by varying the bed material circulation rate from the combustor to the gasifier. Three steady-state operating points were selected from these experiments for further analysis with simulations. These operating points represent the most interesting operating range from the point of view of DME synthesis. The chemical composition of the wood pellets used is presented in Table 2. The operational parameters of the experiments are presented in Table 4. Additional boundary conditions were determined from solid samples for the simulations and are summarised in Table 5. The fuel decomposition fractions (char, tars, and permanent gases) were specified into the model as temperature-dependent. The fractions are summarised in Table 6. The tar fraction of the fuel was evaluated according to gravimetric tar measurements [23]. The char fraction was evaluated based on decomposition experiments presented in Table 3. The permanent gases were calculated from mass balance based on known tar and char fractions from Eq. 2. Moisture and ash content were specified in the model according to standard proximate analysis (Table 2) conducted for the fuel batch on the site. Elemental composition of biomass was specified in the model according to Table 2.

Table 2
Chemical composition of wood pellets used in gasification experiments.

Fuel	Wood pellets
C [wt.%,daf]	50.8
H [wt.%,daf]	6.1
N [wt.%,daf]	0.2
S [wt.%,daf]	0.1
O [wt.%,daf]	42.8
Moisture [wt.%,ar]	6.0
Ash [wt.%,ds]	0.2
LHV [MJ/kg,ar]	17.36

4. Simulation results and discussion

The aim of this work was to develop a fuel model and implement the model into an SEG model frame. By introducing the characteristics of the decomposition phenomena into the model frame, the overall model was able to capture the main characteristics of the SEG process, and aspects about the characteristics are discussed in this section.

4.1. Hydrodynamics and heat balances

The simulations were conducted by introducing the operating parameters of the pilot-scale process into the model with appropriate model equations describing phenomena that are present in the SEG process. A previously developed and validated hydrodynamic scheme was used in the current simulations [9]. Simulated temperature profiles against measurements of the gasifier are shown in Fig. 4. The temperature of the gasifier was adjusted during the experiments by varying the rate of bed material circulation from the combustor to the gasifier. The operating temperature of the gasifier was increased by increasing the circulation rate. Because of uncertainties in the applied boundary conditions, a heat balance correction term was applied to the bed of the gasifier to match local bed temperatures. The heat balance adjustments presented in Table 5 were applied to the bed. A constant heat loss [kW/m] was applied at the freeboard section according to Table 5. The freeboard heat loss was included in the adjustment. This approach is used to compensate for the impact of uncertainties such as devolatilization and uncertainty of the solid flow and temperature measurements in the energy balance.

4.2. Producer gas yield

The typical gas yield range of various SEG experiments is presented in Fig. 5 against the gas yield predicted by the model. The gas yield by the model matches with the typical range. The range is based on literature data [24]. The producer gas composition at the simulated operating points against measurements of the IFK's pilot facility from [3] are shown in Fig. 6. Furthermore, a typical producer gas composition range from various experiments is shown [24]. The range covers various operating conditions and was obtained from experiments with three different gasifiers. As can be seen from Fig. 6, some experiments can

Table 3
Fuel decomposition balances of wood pellets.

Wood pellets	Temperature °C	Liquid yield wt.%,ar	Solid/char yield wt.%,ar	Permanent gas yield wt.%,ar	Moisture wt.%,ar	Ash wt.%,ar	Closure wt.%,ar
	650	36.87	19.43	35.15	-	-	91.45
Temperature	700	31.90	19.52	40.48	-	-	91.90
variation	750	21.09	17.76	51.06	-	-	89.91
	800	20.53	17.28	55.94	-	-	93.75
Standard proximate	905	-	15.29	78.80	5.55	0.36	100

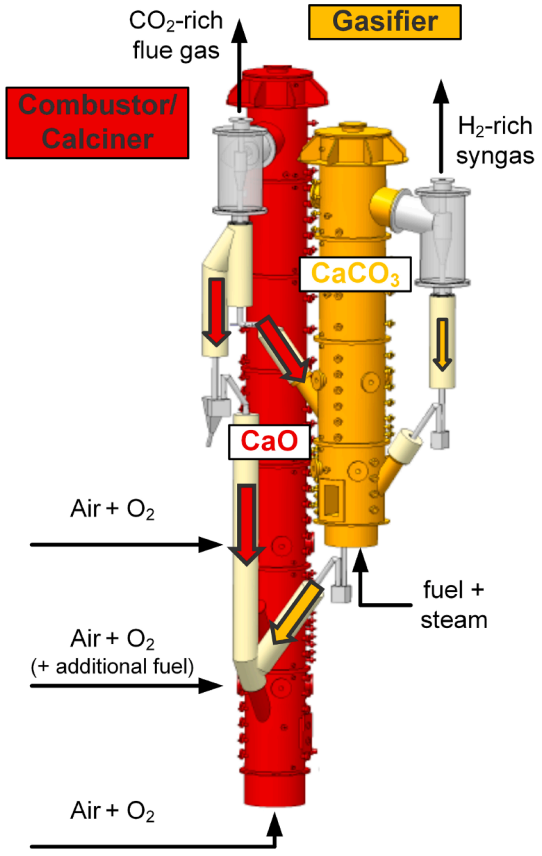

Fig. 3. 200 kW_{th} DFB pilot facility at IFK, University of Stuttgart [9].

Table 4
Operating parameters of gasification experiments.

Parameter	
Biomass feed [kg/h]	30
Steam flow [kg/h]	30.3
Steam temperature [°C]	146
Steam-to-Carbon ratio [mol/mol]	1.5

differ from this range because the producer gas composition is a result of the overall effect of various operating parameters, e.g. bed material circulation rate, steam-to-carbon ratio, and hydrodynamic conditions.

In Table 5, two model parameters for the fuel model are presented. The values for the parameters were determined from gasification experiments. Parameter γ_2 was set based on average distribution of hydrocarbons in the producer gas. Parameter γ_1 was calibrated to the methane concentration in Fig. 6, and a linear fit to the calibration was used.

The producer gas composition from the IFK pilot with respect to operating temperature is shown in Fig. 6. The model was able to predict the main temperature trends for the composition. Furthermore, the

Table 5
Simulation boundary conditions.

Parameter	OP 1.1	OP 1.2	OP 1.3
Operational temperature			
Bed temperature[1] [°C]	710	757	774
Solid circulation from combustor			
Solid flow[1] [kg/h]	498	570	694
Temperature[1] [°C]	734	787	809
Composition			
CaO[1] [wt.%]	93.3	91.2	96.0
$CaCO_3$ [1] [wt.%]	2.0	4.7	0.4
Ash[1] [wt.%]	4.7	4.1	3.6
N_2 sealing gas and purges			
Feed[1] [kg/h]	10.94	15.05	14.63
Temperature			
Freeboard [°C]	200	200	200
Dense Bed [°C]	650	650	650
Fuel model parameters			
γ_1	0.764	0.779	0.785
γ_2	0.642	0.642	0.642
Heat balance			
Freeboard loss [kW/m]	−2.4	−2.4	−2.4
Balance correction [kW/kW_{fuel}]	−0.037	0.072	0.105

[1] Measured value.

Table 6
Temperature-dependent fuel fractions used in the simulations.

OP		1.1	1.2	1.3
Temperature	°C	710	757	774
Tar	wt.%,ds	0.49	0.13	0.13
Char	wt.%,ds	18.33	17.56	17.28
Permanent gas	wt.%,ds	80.98	82.11	82.38
Moisture	wt.%,ar	6.0	6.0	6.0
Ash	wt.%,ds	0.2	0.2	0.2

simulation results with respect to the typical producer gas composition were good. However, there was a deviation between the simulations and measurements of the pilot for CO_2 and H_2 gases. There could be various reasons for the deviation. The modelling was limited within the main reactor, and chemical reactions outside the reactor, e.g. in the cyclones, were not considered. Thus, the modelling could not consider chemical reactions in the cyclones, such as carbonation of the bed material. Another explanation for the deviation could be that the reaction equilibrium of real limestone differs from the thermodynamic reaction equilibrium [25]. Consequently, the CO_2 capture in the pilot could be

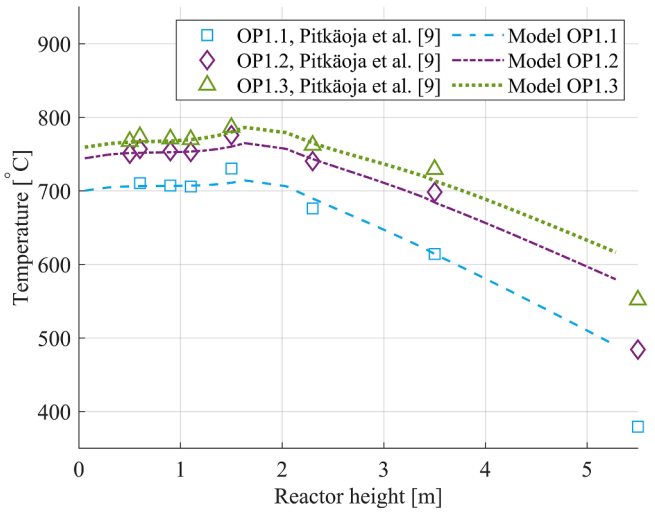

Fig. 4. Simulated temperature profiles against pilot's temperature measurements [9].

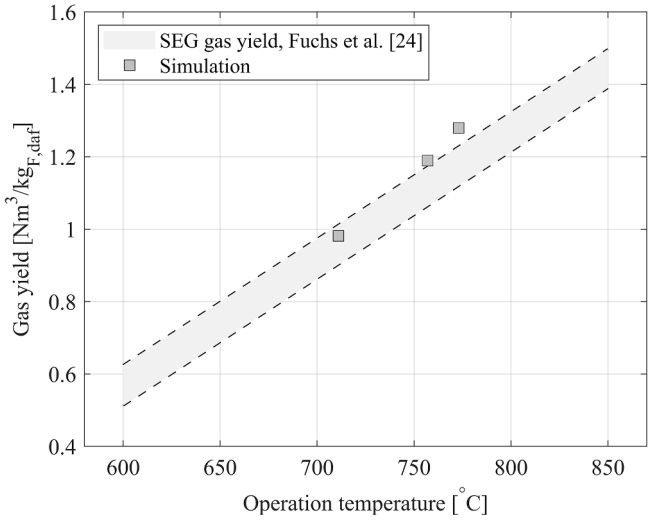

Fig. 5. Gas yield of various SEG experiments and simulated producer gas yield. The gas yield range is based on a data presented by [24].

larger than was predicted by the modelling. Because there is strong coupling of carbonation and water–gas shift, the higher H_2 fraction of the measurements could be explained by an enhanced water–gas shift reaction that was not captured by the modelling. In addition to explanations related to the CO_2 capture, the deviation could be caused by underestimated element transfer from the gasifier to the combustor in the simulations. There could have been material losses that were not included in the modelling and consequently, the model prediction for the CO_2 fractions was higher than the measurements.

The model was able to predict the producer gas composition of IFK experiments with reasonably good accuracy. As indicated, there were uncertainties in the boundary conditions of the experiments, which could explain the model's higher prediction of the CO_2 fractions. Nevertheless, the modelling results were in agreement with the general trends presented in Fig. 5 and Fig. 6. The modelling results were excellent in this respect.

4.3. Bed material CO_2 capture

Bed material CO_2 capture in the gasifier can be determined from the difference in $CaCO_3$ fractions of circulating solids. The bed material $CaCO_3$ mass fraction change in simulations is shown in Fig. 7, with the CO_2 capture determined from the fractions. The bed of the gasifier operated close to the thermodynamic reaction equilibrium. The bed elements with respect to the equilibrium are shown in Fig. 8. The reaction kinetics were fast enough to set the bed operating close to the equilibrium, and therefore the maximum transfer capacity for the CO_2 was attained in each case. Consequently, the operating temperature was the main process parameter to define the amount of carbon capture. The basic operating characteristics are shown in Fig. 7. The CO_2 capture decreases with increasing operating temperature because the maximum transfer capacity is limited by the equilibrium. When the operating temperature was increased to the level of OP 1.3, carbonation was no longer possible owing to thermodynamic limitations of the reaction. Thus, no carbon capture occurred according to Fig. 7. However, Fig. 8 shows that local carbon capture occurred at the upper parts of the bed, but the limestone was calcined before the bottom of the gasifier was reached.

4.4. Carbon balance

Carbon balances were formulated from the simulations for each operating point. The carbon balances were compared against carbon balance data from an SEG balance study [24]. The comparison is shown in Fig. 9. The carbon balances in the figure are presented as the carbon of fuel that is transported from the gasifier to the combustor. The carbon balances by [24] are based on general trends presented in Fig. 5 and Fig. 6.

The total carbon transport (in Fig. 9) was calculated by removing the carbon of the producer gas ($kg_{g,C}/kg_{F,daf,C}$) from the amount of carbon that was fed into the reactor. As a result, 60 wt.% to 40 wt.% of the total carbon was transported to the combustor in the simulations. The total carbon transport to the combustor is very similar in this study and in the study by [24], although there are differences in producer gas yield.

The total carbon transport can be divided among a solid carbon (carbon in char) and $CaCO_3$ to conduct more profound system analysis. The distribution of the carbon fractions is similar in this study and in the study by [24]. However, the simulation showed that the CO_2 transport to the combustor was not possible at the operating temperature of 774 °C owing to thermodynamic limitations. The char of the fuel was almost completely transported to the combustor owing to relatively low residence time in the reactor. Consequently, the carbon transport by the char followed closely the fuel's char fraction from the decomposition balances. Therefore, the elemental carbon concentration of producer gas was mainly the result of devolatilised carbon and carbon capture. This example highlights the importance of the decomposition process for the overall material balance of the SEG.

5. Conclusions

A fuel model for gasification was developed and implemented to an SEG model frame. The fuel model was suitable for various gasification processes and different operating temperatures. The model considered the major decomposition products of the fuel to model the main characteristics of the fuel decomposition. The main elemental balances and influence of temperature on the balances were considered.

The SEG model frame was previously developed based on specifications of a 200 kW_{th} SEG pilot plant [9]. The SEG pilot experiments were simulated with the model frame with the developed fuel model. The modelling focused on a temperature range between 710 °C and 770 °C, with a steam-to-carbon ratio of 1.5 [mol/mol]. This temperature range is the most interesting for the SEG process from the point of view of DME synthesis.

Elemental carbon balances, typical gas yield, and the producer gas composition range of an SEG reactor are presented by [24] for the investigated temperature range. The carbon balances of the simulations were consistent with [24]. Furthermore, the producer gas yield and

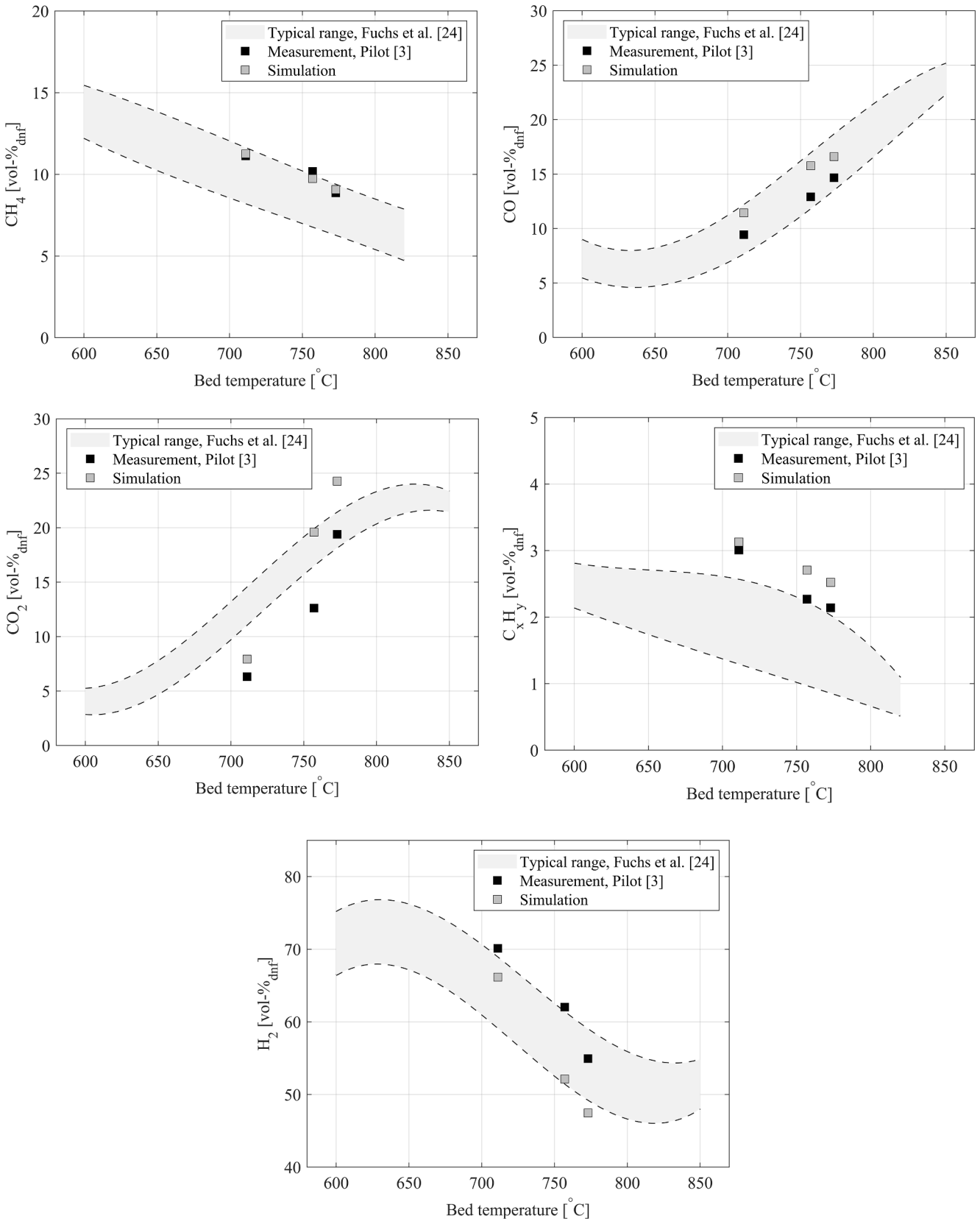

Fig. 6. Volume fractions of H_2, CO, CO_2, CH_4, and C_xH_y gas species of producer gas at the studied operating points of 200 kW_{th} pilot gasifier [3]. The typical range for the measurements is presented based on various SEG experiments [24].

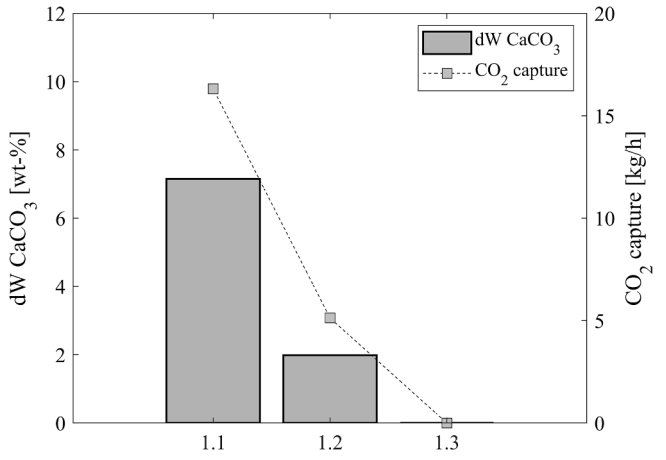

Fig. 7. Bed material $CaCO_3$ mass fraction change within the gasifier and CO_2 capture.The mass fraction change $dWCaCO_3$ is calculated as a difference of $CaCO_3$ fractions of solid inflow and solid outflow.

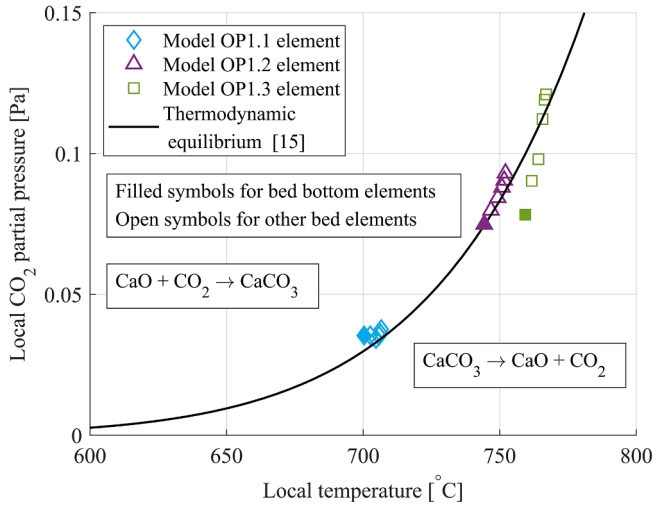

Fig. 8. Simulated local CO_2 partial pressure in the bed elements with respect to the local temperature. The pressure in emulsion is presented. The thermodynamic reaction equilibrium according to [15] is shown for comparison.

composition followed the typical trends. The heat balances of the model were in agreement with the trends from the IFK pilot reactor. Overall, the performance of the model was good. The model produced the main phenomena of the SEG process. Thus, the model can be used to study the operational characteristics of the process. The model predicted with reasonably good accuracy the CO, CO_2, C_xH_y, CH_4, and H_2 gas fractions of the IFK experiments. The simulated volume fractions of carbon-based gases were higher than the measurements. This indicates the carbon concentration of the producer gas to be higher than that of the pilot. This may be due to material losses during the experiments that were not specified in the model. Fuel decomposition balances played an important role in the overall balances of the process. Therefore, it is important to model the main phenomena of the fuel decomposition process. The decomposition has a significant impact on the element transfer between the reactors and for the composition of the producer gas.

To investigate material losses and fuel decomposition balances further, the element exchange between the gasifier and the combustor must be determined. The element exchange can be estimated by formulating a balance study. The known element exchange opens the possibility to evaluate the pilot system more profoundly and elucidates the uncertainties, such as the material losses.

The work presented in this paper improves the current

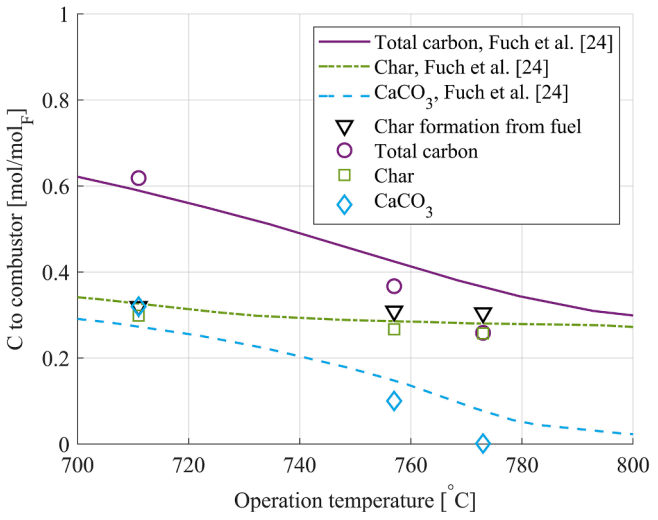

Fig. 9. Carbon transport to the combustor. The carbon transport of the model is presented against balances from an SEG balance study [24]. The overall carbon flow to the combustor is divided among char and $CaCO_3$. The char fraction of the fuel is shown for comparison.

understanding of the physical and chemical phenomena governing the SEG processes. Further investigations on this topic could include a balance study of the pilot SEG reactor system to evaluate the element exchange between the reactors. An understanding of material exchange in complex reactor systems is important for analysing the operation of the systems and for modelling the processes.

CRediT authorship contribution statement

Antti Pitkäoja: Methodology, Software, Formal analysis, Writing - original draft, Visualization, Validation. **Jouni Ritvanen:** Methodology, Software, Writing - review & editing, Supervision, Visualization. **Selina Hafner:** Investigation, Writing - review & editing, Visualization. **Timo Hyppänen:** Writing - review & editing, Supervision. **Günter Scheffknecht:** Writing - review & editing, Supervision.

Declaration of Competing Interest

The authors declare that they have no known competing financial interests or personal relationships that could have appeared to influence the work reported in this paper.

Acknowledgements

This work in FLEDGED project has received funding from the European Union's Horizon 2020 research and innovation programme under grant agreement No. 727600.

References

[1] Delbeke J, Vis P. EU Climate Policy Explained. Routledge; 2016.
[2] L. Pelkmans, European Union - 2018 update, Bioenergy policies and status of implementation, Technical Report, IEA Bioenergy, 2018. https://www.ieabioenergy.com/wp-content/uploads/2018/10/CountryReport2018_EU_final.pdf.
[3] Hafner S, Spörl R, Scheffknecht G. Sorption Enhanced Gasification: Process validation and investigations on the syngas composition in a 200 kW th dual fluidized bed facility. In: 23rd International Conference on Fluidized Bed Conversion; 2018. p. 826–32.
[4] Fiaschi D, Michelini M. A two-phase one-dimensional biomass gasification kinetics model. Biomass Bioenergy 2001;21:121–32.
[5] Hejazi B, Grace J, Bi X, Mahecha-Botero A. Kinetic Model of Steam Gasification of Biomass in a Bubbling Fluidized Bed Reactor. Energy Fuels 2017;31:1702–11.
[6] Kaushal P, Abedi J, Mahinpey N. A comprehensive mathematical model for biomass gasification in a bubbling fluidized bed reactor. Fuel 2010;89:3650–61.

[7] Di Blasi C, Signorelli G, Di Russo C, Rea G. Product Distribution from Pyrolysis of Wood and Agricultural Residues. Ind Eng Chem Res 1999;38:2216–24.
[8] Neves D, Thunman H, Matos A, Tarelho L, Gómez-Barea A. Characterization and prediction of biomass pyrolysis products. Progress Energy Combust Sci 2011;37:611–30.
[9] Pitkäoja A, Ritvanen J, Hafner S, Hyppänen T, Scheffknecht G. Simulation of a sorbent enhanced gasification pilot reactor and validation of reactor model. Energy Conversion Manage 2020;204:112318.
[10] Myöhanen K. Modelling of Combustion and Sorbent Reactions in Three-Dimensional Flow Environment of a Circulating Fluidized Bed Furnace. Acta Universitatis Lappeenrantaensis. Doctoral Dissertation, Lappeenranta 2011.
[11] Gómez-Barea A, Leckner B. Modeling of biomass gasification in fluidized bed. Progress Energy Combust Sci. 2010;36:444–509.
[12] Tuomi S, Kurkela E, Simell P, Reinikainen M. Behaviour of tars on the filter in high temperature filtration of biomass-based gasification gas. Fuel 2015;139:220–31.
[13] Martínez I, Grasa G, Murillo R, Arias B, Abanades J. Kinetics of calcination of partially carbonated particles in a Ca-looping system for CO2 capture. Energy Fuels 2012;26:1432–40.
[14] Fang F, Li Z-S, Cai N-S. Experiment and Modeling of CO 2 Capture from Flue Gases at High Temperature in a Fluidized Bed Reactor with Ca-Based Sorbents. Energy Fuels 2009;23:207–16.
[15] Stanmore B, Gilot P. Review-calcination and carbonation of limestone during thermal cycling for CO2 sequestration. Fuel Process Technol 2005;86:1707–43.
[16] Shimizu T, Hirama T, Hosoda H, Kitano K, Inagaki M, Tejima K. A Twin Fluid-Bed Reactor for Removal of CO2 from Combustion Processes. Chem Eng Res Des 1999;77:62–8.
[17] Alonso M, Rodríguez N, Grasa G, Abanades J. Modelling of a fluidized bed carbonator reactor to capture CO2 from a combustion flue gas. Chem Eng Sci 2009;64:883–91.
[18] Rajan R, Wen C. A comprehensive model for fluidized bed coal combustors. AIChE J 1980;26:642–55.
[19] Risnes H, Sorensen L, Hustad J. CO2 reactivity of chars from wheat, spruce and coal. In: Bridgewater A, editor. Progress in Thermochemical Biomass Conversion. Oxford: Blackwell Science; 2001. p. 61–72.
[20] Hemati M, Laguerie C. Determination of the kinetics of the sawdust steam-gasification of charcoal in a thermobalance. Entropie 1988;142:29–40.
[21] Biba V, Macák J, Klose E, Malecha J. Mathematical Model for the Gasification of Coal under Pressure. Ind Eng Chem Process Design Dev 1978;17:92–8.
[22] de Souza-Santos M. Comprehensive modelling and simulation of fluidized bed boilers and gasifiers. Fuel 1989;68:1507–21.
[23] Hafner S, Schmid M, Spörl R, Scheffknecht G. Experimental Investigation of the Sorption Enhanced Gasification of Biomass in a Dual Fluidized Bed Pilot Plant. In: 27th European Biomass Conference & Exhibition; 2019.
[24] Fuchs J, Schmid JC, Müller S, Mauerhofer AM, Benedikt F, Hofbauer H. The impact of gasification temperature on the process characteristics of sorption enhanced reforming of biomass. Biomass Conver Biorefinery 2019.
[25] Florin NH, Harris AT. Enhanced hydrogen production from biomass with in situ carbon dioxide capture using calcium oxide sorbents. Chem Eng Sci 2008;63:287–316.